fcc antiferromagnetic Ising model in a uniform external field solved by mean-field theory

A. D. Beath and D. H. Ryan
Physics Department and Centre for the Physics of Materials, McGill University, 3600 University Street, Montreal, Quebec, Canada H3A 2T8
(Received 11 February 2005; revised manuscript received 18 May 2005; published 21 July 2005)

The fcc antiferromagnetic Ising model with nearest-neighbor interactions in a uniform external field is studied using a simple mean-field theory, and a phase diagram is presented. Our theory is formulated in the spirit of a Weiss-like molecular field theory: Four spins forming a basic tetrahedron are allowed to fluctuate while the surrounding 28 spins take mean-field values. The phase diagram is similar to that obtained in the Bragg-Williams approximation for chemical ordering of $Cu_{1-x}Au_x$ alloys, although apart from the similar phase diagrams, the two theories give substantially different results. First, all of the detected transitions are correctly predicted to be first order. Second, we obtain two previously undetected reentrant phases. The existence of reentrant phases is discussed and we show that this ordering scenario is fully consistent with the results of the Bragg-Williams approximation which does *not* contain reentrant phases.

DOI: 10.1103/PhysRevB.72.014455 PACS number(s): 75.10.Hk, 64.60.Cn, 64.60.Kw

I. INTRODUCTION

Frustrated magnetism presents one of the most difficult challenges to our understanding of magnetic order, as exemplified by the ongoing controversy regarding spin glass order. Frustration—the inability to simultaneously satisfy all interactions—leads to nontrivial, highly degenerate ground states, and it can be very difficult to ascertain the correct solution to a given model even when extreme approximations are used, such as mean-field theory. The only nontrivial frustrated model which has been solved exactly[1] is the two-dimensional Ising antiferromagnet on a triangular lattice (t-IAF) by extension of the celebrated Onsager solution[2] of the two-dimensional Ising ferromagnet. The principal result is that no finite temperature ordering occurs so that the effect of frustration is to increase the lower critical dimension beyond two. Since the exact solution to the t-IAF problem is known, it is a good starting point for testing approximate theories prior to application to more complex problems. A particularly good mean-field theory, the loopwise (LS) scheme, was recently used to study the t-IAF by Galam[3] and gave the correct solution: The Néel temperature (T_N) is zero as in the exact solution.

The most natural extension of the mean-field theory of Galam beyond the t-IAF is to the three-dimensional fcc Ising antiferromagnet (fcc-IAF). However, for the fcc-IAF the exact solution is, of course, unknown and the form of the phase diagram in a uniform external field H remains a considerable problem.[4] The LS scheme easily accommodates a magnetic field so that application to the fcc-IAF is useful in providing a better understanding of the fcc-IAF model. In addition, the fcc-IAF model provides an important test of the strength and validity of the LS scheme when applied to frustrated models, which are more difficult than the t-IAF. We also note that nearly all calculations of the fcc-IAF model are solutions of the alloy phase diagram, which cannot yield the magnetic phase diagram. By contrast, solutions of the magnetic phase diagram, immediately yield the corresponding alloy phase diagram, making the calculation of the magnetic problem more versatile.

The fcc-IAF model consists of Ising spins which can take the values $S_i=\pm 1$ located at the vertices of an fcc lattice interacting with nearest-neighbor antiferromagnetic bonds $J=-1$. The Hamiltonian in a uniform external field H is

$$\mathcal{H}=-J\sum_{\langle i,j\rangle} S_iS_j - H\sum_i S_i, \tag{1}$$

where the summation $\langle i,j\rangle$ runs over all nearest-neighbor pairs. The fcc lattice can be built from four interpenetrating simple cubic (SC) lattices, and the nearest-neighbor spins of each site in one simple cubic lattice are four spins from each of the remaining three SC lattices. Due to the symmetry of the ordered phases of the fcc-IAF, it is easiest to consider the lattice as being built out of basic tetrahedra which contain one spin from each of the four SC lattices. The average values of the spins in each basic tetrahedron are then the sublattice magnetizations: $m_k=\langle S_k\rangle$ with $k=1$, 2, 3, and 4 and the average magnetization is just $m=\frac{1}{4}\Sigma_k m_k$.

At zero temperature, minimization of the Hamiltonian gives the ground states, which are well known.[5] In what follows we consider $H\geqslant 0$ since the phase diagram is symmetric about $H=0$. For $0\leqslant H<4$ the ground state is denoted AB (borrowed from the alloy language for $Cu_{1-x}Au_x$ ordering) exhibiting antiferromagnetic (AF) order within successive (100) planes but with no correlation between the planes:[6] Any AF plane may have all its spins flipped at zero energy cost. The ground-state energy/spin, E, in the AB phase is just -2, and is independent of the field H. For $4<H<12$ the ordering is denoted A_3B and successive planes are ordered AF/FM/AF/FM, etc.—where FM refers to ferromagnetic order—again with no correlation between the AF planes. The ground-state energy/spin is $E=-\frac{1}{2}H$. For $H>12$, the ground state is A (the paramagnetic phase for $T>0$) with all spins ordered "up" along the field direction, and the ground-state energy/spin is $E=6-H$. At zero temperature ($T=0$), the critical field $H_c^1=4$ separates the AB and A_3B phases while the critical field $H_c^2=12$ separates the A_3B and

 ©2005 The American Physical Society

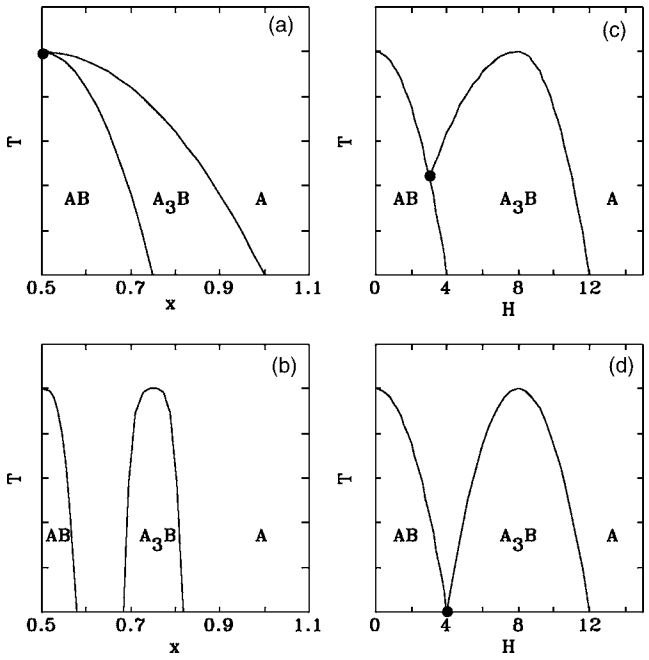

FIG. 1. Schematic phase diagrams for the fcc-IAF model obtained in (a) the Bragg-Williams approximation (Ref. 8), (b) the quasichemical approximation (Ref. 9), (c) the Kikuchi approximation (Refs. 16 and 17) and most recent Monte Carlo result (Ref. 4), and (d) early Monte Carlo result (Ref. 5).

A phases. At the critical fields H_c^1 and H_c^2 other structures[5,7] may become ground states, but we do not explore this possibility here.

For $T>0$ the phase diagram is much less clear. A variety of approximate methods and Monte Carlo methods[4,5] have been used to study the problem. The first treatment of a simplified version of the fcc-IAF model was given by Shockley[8] more than 60 years ago using the Bragg-Williams approximation to describe the chemical ordering of $Cu_{1-x}Au_x$ alloys. In the magnetic language spin "up" refers to one chemical species and spin "down" refers to the other such that the magnetization is proportional to the concentration x of chemical species. In Shockley's treatment however, a clear magnetic analog cannot be deduced since the concentration x is conserved in the alloy problem while in the magnetic problem it is not. A schematic phase diagram in the x-T plane is shown in Fig. 1(a). The principle results are (i) all transitions are first order except at $x=\frac{1}{2}$ ($H=0$), and (ii) there is a multicritical point at $x=\frac{1}{2}$ where the paramagnetic A phase and ordered AB and A_3B phases occur simultaneously. In $Cu_{1-x}Au_x$, all of the transitions are first order, in agreement with Shockley's treatment, except at $x=\frac{1}{2}$, while the multicritical point does not occur at $x=\frac{1}{2}$.

Other methods have been used to study the model with various disparate solutions. As far as mean-field theory is concerned, all attempts meet failure. The pair approximation yields no finite temperature ordering.[10] The Bethe scheme[11] for fcc lattices, sometimes erroneously considered equivalent to the pair approximation in giving no ordering.[5] does yield finite T ordering.[12,13] However, as shown by Galam,[14] the Bethe scheme violates the intrinsic symmetry of the lattice and cannot therefore be considered a valid solution for cubic lattices. Renormalization-group calculations yield no finite T order in the AB phase, but do find finite T order in the A_3B phase.[15] The quasichemical method yields finite T order in both phases, yet there is a gap between phases where no finite T order occurs[9] as shown in Fig. 1(b). A more sophisticated approximation,[10] the Kikuchi approximations in both the tetrahedral[16,17] and the tetrahedral-octahedral[18] approximations, yields first-order transitions, and the multicritical point occurs at finite temperature and finite field [shown schematically in Fig. 1(c)]. However, increasingly accurate approximations move the multicritical point to lower temperatures and fields, possibly even to the $T=0$ ground-state value $H_c^1=4$ [Fig. 1(d)]. For many years this result seemed quite satisfactory since the best available Monte Carlo phase diagram,[5] shown in Fig. 1(d), placed the multicritical points at $H_c^1=4$ at $T=0$. However, using larger system sizes it appears that the older result is likely a finite-size effect, and the Monte Carlo results now agree[4] with the phase diagram given in Fig. 1(c), placing the multicritical point at finite T and H. On the other hand the Monte Carlo results contain hysteresis, which can severely complicate the determination of the phase diagram.

Our treatment of the problem here is within the framework of mean-field theory. The Hamiltonian, Eq. (1), is simplified so that a fraction $f=\frac{1}{8}$ of the spins fluctuate while the others do not. We evaluate the partition function, and calculate averages, with the states of the system weighted according to their Boltzmann weights. A further simplification of the problem is made by only considering the A, AB, and A_3B states since only these states are found in the Monte Carlo results[4,5] and the Kikuchi method.[16,17] While states such as A_3B are found to split into A_2BC—three sublattice magnetizations, one of which is shared by two sublattices—at low temperatures in the Bragg-Williams approximation[8] and could in principle appear here, the emergence of such states cannot change the overall structure of the phase diagram we have found.

II. SETTING UP THE MEAN-FIELD THEORY

Any mean-field theory (MFT) begins with replacing the Hamiltonian of the full problem with some suitable approximation. In the LS scheme proposed by Galam[3,14] half of the spins fluctuate while the other half take mean-field values. The method was devised since it was realized that Bethe's mean-field theory violated the intrinsic symmetry of the lattice, and that this violation may result in incorrect solutions. Here, as Galam states,[3] we do not propose that a correct MFT will give the correct transition temperatures or critical exponents, but that the theory should yield solutions which are consistent with the lower critical dimension of the problem. Simple Weiss MFT in this sense fails since finite temperature transitions occur in all dimensions greater than zero while Bethe's MFT yields the correct lower critical dimension in ferromagnetic, frustration-free, models. However, it cannot be a valid solution to *any* problem with cubic symmetry.[14]

To apply the LS scheme to the fcc-IAF, it is necessary to alter slightly the prescription given by Galam where the lat-

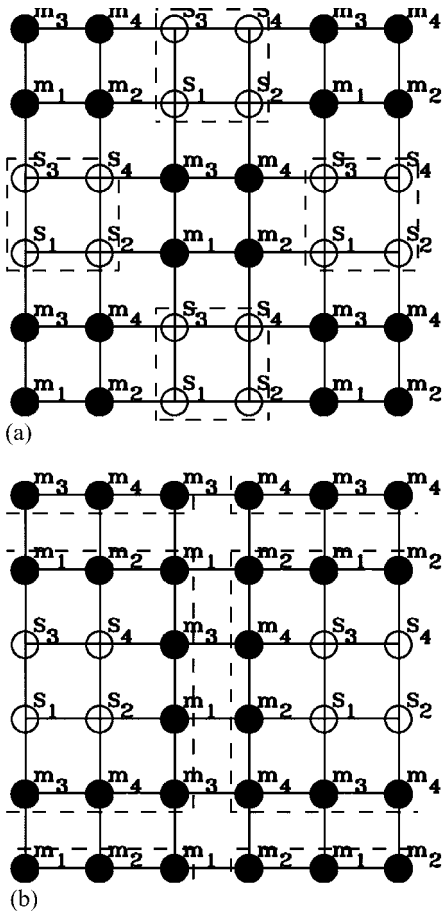

FIG. 2. Division of a square lattice into (a) loopwise scheme (LS) of Galam and (b) theory presented here. Fluctuating spins in loop k, s_i^k, are surrounded by dashed lines while m_i denote mean-field spins.

tice is decomposed into two sublattices, one of which fluctuates while the other takes mean-field values. First, consider the square lattice illustrated in Fig. 2(a). In the LS scheme, it is clear that if one wishes to decompose the lattice into k loops, there are mean field spins m_i which couple to fluctuating spins S_j^k in different loops. Therefore, the Hamiltonian will contain terms like $m_2(S_1^k+S_4^{k'})$ with $k \neq k'$. In Galam's work, these terms are not strictly neglected: Spins in different loops are treated identically and $S_i^k = S_i^{k'}$. Therefore, when the summation over states is taken in order to evaluate the partition function the set of spins in different loops are always in the same state. If instead we take the summation over *all* states, then the problem is equivalent to a two-dimensional Ising model in a magnetic field and the problem has actually become harder to solve. To overcome this difficulty we consider a fluctuating set of spins surrounded by mean-field spins so that there are no m_i^k which couple to fluctuating spins $S_i^{k'}$ with $k \neq k'$ as shown in Fig. 2(b). Then, within the mean-field approximation, the full summation over all states can be carried out.

In our application of this MFT we have chosen to decompose the lattice of linear dimensions L, containing $N=4L^3$ spins, into M blocks of 32 spins such that the lattice now

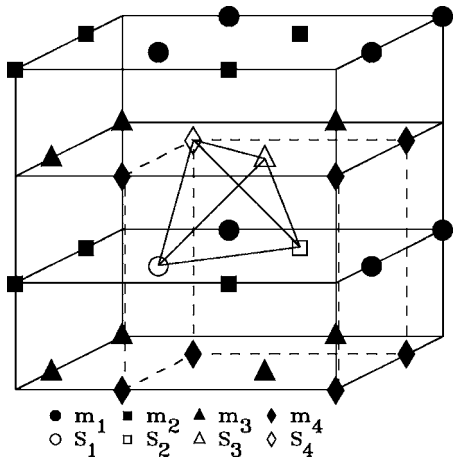

FIG. 3. Division of the fcc lattice into fluctuating spins S_i and mean-field spins m_i for the MFT presented here. The cell contains 32 sites, four of which fluctuate. Fluctuating spins S_i form a tetrahedron at the center of the cell. Dashed line shows the fcc unit cell.

consists of $M=N/32$ blocks. The central four spins forming a basic tetrahedron are allowed to fluctuate, while the surrounding 28 spins take mean-field values, illustrated in Fig. 3. Since we have M blocks and each block has 16 states, the summation over all states contains 16^M states. The Hamiltonian is now a sum of block Hamiltonians $\mathcal{H}_k$. Each $\mathcal{H}_k$ can be considered to be the sum of three parts:

(i) The interaction between neighboring fluctuating spins and the fluctuating spins with the field, $\mathcal{H}_k^{S-S}$,

$$\mathcal{H}_k^{S-S} = -\frac{J}{2}[S_1(S_2+S_3+S_4)+S_2(S_3+S_4+S_1)+S_3(S_4+S_1+S_2)+S_4(S_1+S_2+S_3)]-H(S_1+S_2+S_3+S_4), \quad (2)$$

(ii) the interaction between mean-field spins m_i and the fluctuating spins S_i, $\mathcal{H}_k^{S-m}$,

$$\mathcal{H}_k^{S-m} = -\delta_I J[S_1(m_2+m_3+m_4)+S_2(m_3+m_4+m_1)+S_3(m_4+m_1+m_2)+S_4(m_1+m_2+m_3)], \quad (3)$$

and (iii) the interaction between neighboring mean-field spins m_i and between the m_i and the field, $\mathcal{H}_k^{m-m}$,

$$\mathcal{H}_k^{m-m} = -\delta_S\frac{J}{2}[m_1(m_2+m_3+m_4)+m_2(m_3+m_4+m_1)+m_3(m_4+m_1+m_2)+m_4(m_1+m_2+m_3)] - 7H(m_1+m_2+m_3+m_4), \quad (4)$$

where $\delta_I=3$ and $\delta_S=25$ account for the coupling between $S-m$ and $m-m$, respectively. The mean-field Hamiltonian is

$$\mathcal{H} = \sum_k (\mathcal{H}_k^{S-S} + \mathcal{H}_k^{S-m} + \mathcal{H}_k^{m-m}). \quad (5)$$

With the modified mean-field Hamiltonian [Eq. (5)] it is now possible to calculate the partition function, as well as many important averages. The partition function for the infinite lattice, with $\beta=1/k_BT$, is now

$$Z = \sum_{S_i=\pm 1} e^{-\beta\mathcal{H}} = \left(\sum_{S_i^k=\pm 1} e^{-\beta\mathcal{H}} \right)^M = (Z_k)^M, \tag{6}$$

where Z_k is the partition function for a single block k, and $\Sigma_{S_i^k}$ means a summation over the fluctuating spins forming the tetrahedron at the center of block k. Average values of a thermodynamic quantity X are calculated in the usual way

$$\langle X \rangle = \frac{\sum_s X(s)P(s)}{\sum_s P(s)}, \tag{7}$$

where Σ_s is a sum over all states and $P(s)$ is the probability of any given state of the system s. For instance, the sublattice magnetizations are

$$\langle S_i^k \rangle = \frac{1}{Z}\left(\sum_{S_i=\pm 1} S_i^k e^{-\beta\mathcal{H}} \right)$$

$$\langle S_i^k \rangle = \frac{1}{Z_k}\left(\sum_{S_i^k=\pm 1} S_i^k e^{-\beta\mathcal{H}^k} \right), \tag{8}$$

where in the second line it is clear that the average value of a spin in block k only depends upon the fluctuating spins in block k, as well as the mean-field magnetizations. Thus, by constructing our blocks such that there are no m values that couple to both a S_i^k and a $S_j^{k'}$, with $k \neq k'$, average values such as $\langle S_i^k \rangle$ depend only on the fluctuating spins in block k. Symmetry is then restored by demanding self-consistency, i.e., $m_i = \langle S_i \rangle$. Other average values can also be calculated quite easily, once the four sublattice magnetizations m_i have been determined.

III. SOLVING THE MEAN-FIELD THEORY

To solve the problem we need to calculate the partition function [Eq. (6)] as well as the four spin averages $\langle S_i \rangle$. The partition function is

$$Z_k = [X^{12}(A^6Y^4 + A^{-6}Y^{-4}) + A^2BY^2 + A^{-6}CY^{-2} + X^{-4}A^{-2}D]Z_k^{mm}, \tag{9}$$

where we have used the following abbreviations:

$$A = x_1x_2x_3x_4, \tag{10}$$

$$B = x_1^4 + x_2^4 + x_3^4 + x_4^4, \tag{11}$$

$$C = (x_1x_2x_3)^4 + (x_1x_2x_4)^4 + (x_1x_3x_4)^4 + (x_2x_3x_4)^4, \tag{12}$$

$$D = (x_1x_2)^4 + (x_1x_3)^4 + (x_1x_4)^4 + (x_2x_3)^4 + (x_2x_4)^4 + (x_3x_4)^4, \tag{13}$$

and $x_i = \exp(K\delta_I m_i)$, $X = \exp(K)$, $Y = \exp(\beta H)$, and $K = \beta J/2$. The term Z_k^{mm} is a common factor occurring in the partition function that does not depend explicitly upon the state of the S_i^k

$$Z_k^{mm} = \exp[2K\delta_S(m_1m_2 + m_1m_3 + m_1m_4 + m_2m_3 + m_2m_4 + m_3m_4) + 7\beta H(m_1 + m_2 + m_3 + m_4)]. \tag{14}$$

The spin average is also straightforward, if tedious. The result is:

$$\langle S_i^k \rangle = \frac{Z_k^{mm}}{Z_k}\{X^{12}[A^6Y^4 - A^{-6}Y^{-4}] + A^2[B - 2x_i^4]Y^2 - A^{-6}[C - 2A^4x_i^{-4}]Y^{-2} + X^{-4}A^{-2}[D - 2x_i^4(B - x_i^4)]\}. \tag{15}$$

Equation (15) allows us to locate the zero-field transitions temperatures for both the AB solution of the antiferromagnetic model ($J=-1$) and the FM solution of the ferromagnetic model ($J=+1$). For the ferromagnetic model an expansion in m, with $m_1=m_2=m_3=m_4=m$, yields the following equation:

$$36\beta_C(e^{6\beta_C} + 1) = e^{6\beta_C} + 4 + 3e^{-2\beta_C}, \tag{16}$$

with $\beta_C^{-1} = k_BT_C$. Taking $k_B=1$ we get $T_C = 11.7189\ldots$, only slightly improved from the Weiss MFT result $T_C=12$ and, not unexpectedly, still quite far from the estimate[14] $T_C = 9.7943$. For the antiferromagnetic model ordering AB we have $m_1=m_2=-m_3=-m_4=m$, and a small m expansion yields

$$24\beta_N(e^{2\beta_N} + 1) = 6e^{2\beta_N} + 8 + 2e^{-6\beta_N}, \tag{17}$$

and we get $T_N = 3.5025\ldots$, a large reduction compared to T_C for the ferromagnetic model, but still quite far from the Monte Carlo estimate[5] $T_N = 1.76$. Also note that one immediately gets the high-temperature paramagnetic limit $\langle S_i \rangle = 0$ as $\beta \to 0$ for any finite H.

Lastly, the energy/spin can be written as the sum of two contributions,

$$\langle E \rangle = \frac{1}{32}(\langle E^s \rangle + \langle E^m \rangle), \tag{18}$$

where the first depends upon the state of the fluctuating spins and the second does not. The second term $\langle E^m \rangle$ is easy to calculate since all of the dependence on $P(s)$ cancels through division by Z, and

$$\langle E^m \rangle = -J\delta_S(m_1m_2 + m_1m_3 + m_1m_4 + m_2m_3 + m_2m_4 + m_3m_4) - 7H(m_1 + m_2 + m_3 + m_4). \tag{19}$$

The first term $\langle E^S \rangle$ like $\langle S_i \rangle$, depends upon $P(s)$, and is thus more complex to calculate. The result is

$$\langle E^s \rangle = \frac{Z_k^{mm}}{Z_k}\Bigg[-X^{12}A^6Y^4(6J + 4H + 12J\delta_I m) - X^{12}A^{-6}Y^{-4}(6J - 4H - 12J\delta_I m) - A^2Y^2\left(B(2H + 4\delta_I Jm) + 2\delta_I J\left(\sum_i m_i x_i^4 \right) \right) + A^{-2}Y^{-2}\left(A^{-4}C(2H + 4\delta_I Jm) + 2\delta_I J\left(\sum_i m_i x_i^{-4} \right) \right) + X^{-4}A^{-2}\left(2JD - \delta_I J\left(\sum_i m_i\left(2x_i^4(B - x_i^4) - D \right) \right) \right) \Bigg], \tag{20}$$

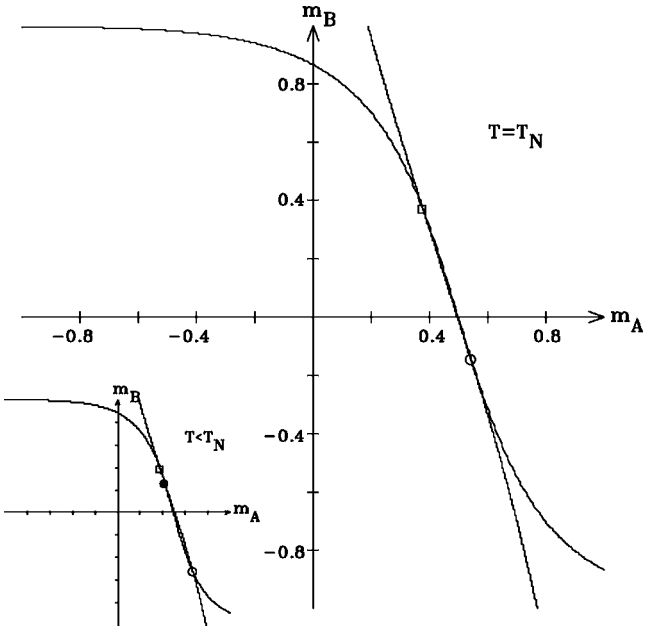

FIG. 4. Solutions to Eqs. (22) and (23) for $T=T_N$ in the A_3B phase for $H=6$. The crossing point □ is the paramagnetic A solution, and the crossing point ○ is the ordered A_3B solution. Inset shows same plot for $T<T_N$, which shows □ the paramagnetic solution, ○ the A_3B ordered state, and ● the alternate ordered A_3B state which has a free energy intermediate to both □ and ○.

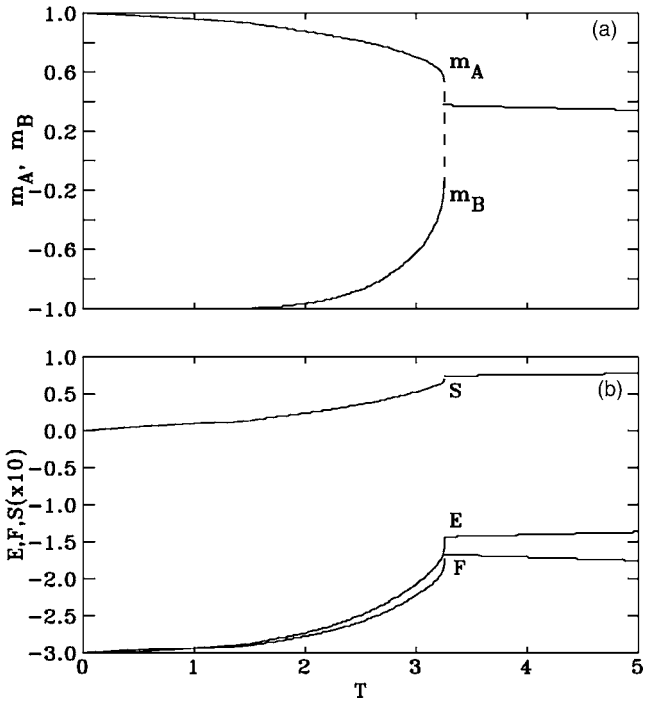

FIG. 5. Some interesting thermodynamic quantities in the ordered A_3B phase for $H=6$. The sublattice magnetizations m_A and m_B are shown in (a). In (b) we show, from top to bottom, the entropy/site, energy/site, and free energy/site.

where we have abbreviated $m=\frac{1}{4}(m_1+m_2+m_3+m_4)$.

The problem now involves restoring the symmetry initially lost by allowing a fraction of the spins to fluctuate while the rest do not. This requires solving Eq. (15) subject to the constraint that $m_i=\langle S_i\rangle$ for the various ordered states. For the AB state we have $m_1=m_2=m_A$ and $m_3=m_4=m_B$, and permutations. Note that Eq. (15) is invariant with respect to which permutation is used. Thus for the AB phase we must solve simultaneously two transcendental equations. For the A_3B phase we have $m_1=m_2=m_3=m_A$ and $m_4=m_B$, again requiring the simultaneous solution of two transcendental equations. For each of the phases AB and A_3B, there is always a solution corresponding to $m_A=m_B$; the paramagnetic solution. Ordered solutions appear in much the same way as in the Weiss molecular field result.

Once we have obtained both the paramagnetic solution and the ordered solutions, the stable solution is that which minimizes the free energy. Thus, for every solution which is found in each ordered phase we need to calculate the free energy/site from the relation

$$F=-\frac{k_BT}{32M}\ln(Z)=-\frac{k_BT}{32}\ln(Z_k). \tag{21}$$

Since the free energy is also given by $F=E-TS$, and we can calculate the energy/site from Eq. (18), the entropy/site S follows immediately. Indeed, from explicitly calculating Z at zero temperature assuming perfectly ordered AB, A_3B, and A states (i.e., all $m_i=\pm1$), one recovers the energy/site given in the introduction, since $F=E$ when $T=0$.

IV. SOLVING THE TRANSCENDENTAL EQUATIONS

To find solutions in the ordered AB and A_3B phases we must solve two transcendental equations simultaneously. For the A_3B phase we have $\langle S_1\rangle=\langle S_2\rangle=\langle S_3\rangle=m_A$ and $\langle S_4\rangle=m_B$. Eq. (15) then gives two transcendental equations

$$m_A=\mathcal{M}_A^{A_3B}(m_A,m_B,\beta,H), \tag{22}$$

$$m_B=\mathcal{M}_B^{A_3B}(m_A,m_B,\beta,H), \tag{23}$$

to be solved self-consistently. In Fig. 4 we have plotted the solutions of Eqs. (22) and (23) for $T=T_N$ and $T<T_N$ for $H=6$. For $T>T_N$ there is one paramagnetic solution with $m_A=m_B$. For $T<T_N$ there are three solutions, one paramagnetic solution and two ordered solutions. The ordered solutions are not related by time-reversal symmetry for $H\neq0$. As can be seen from the solutions of Eqs. (22) and (23) at $T=T_N$, shown in Fig. 4, there is a finite jump in the sublattice magnetizations at T_N. In Fig. 5 we have plotted (i) the sublattice magnetizations for the paramagnetic and antiferromagnetic states and (ii) the energy/site [Eq. (18)] in both A and A_3B states, the free energy/site [Eq. (21)] and the entropy/site $[S=(E-F)/T]$.

In the case of the AB phase we have $\langle S_1\rangle=\langle S_2\rangle=m_A$ and $\langle S_3\rangle=\langle S_4\rangle=m_B$. Equation (15) then gives the two transcendental equations

$$m_A=\mathcal{M}_A^{AB}(m_A,m_B,\beta,H), \tag{24}$$

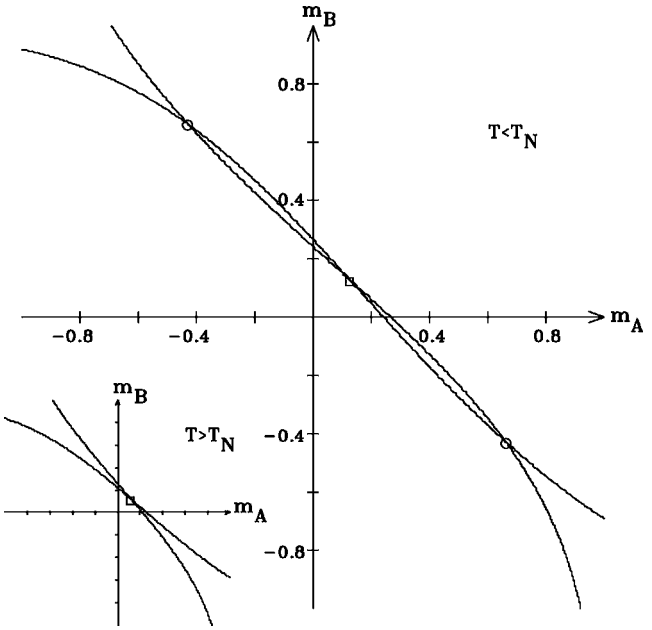

FIG. 6. Solutions to Eqs. (24) and (25) for $T<T_N$ in the AB phase for $H=2$. The crossing point □ is the paramagnetic A solution, and the crossing points ○ are the two ordered AB solutions. Inset shows same plot for $T>T_N$, which shows only paramagnetic A solutions.

$$m_B = \mathcal{M}_B^{AB}(m_A, m_B, \beta, H), \tag{25}$$

which must be solved self-consistently. In Fig. 6 we have plotted the solutions of Eqs. (24) and (25) for $T>T_N$ and $T<T_N$ for $H=2$, and the intersections give the sublattice magnetizations in the AB state. For $T>T_N$ there is one solution, $m_A=m_B$, which is the paramagnetic solution. For $T<T_N$ there are three solutions corresponding to two ordered AB phases, related via time-reversal symmetry, as well as the paramagnetic phase. The sublattice magnetization of the AB solution is continuous, unlike that of the A_3B phase. In Fig. 7 we have plotted (i) the sublattice magnetizations for the paramagnetic and antiferromagnetic states and (ii) the energy/site [Eq. (18)] in both A and AB states, the free energy/site [Eq. (21)] and the entropy/site $[S=(E-F)/T]$.

V. PHASE DIAGRAM

Using the free energies of the paramagnetic A phase and the ordered AB and A_3B phases, a phase diagram is readily constructed. The H-T phase diagram is shown in Fig. 8. The corresponding x-T phase diagram, as will be shown, is equivalent to the one illustrated in Fig. 1(a) and so is qualitatively identical to the Bragg-Williams phase diagram.

At $T=0$, the ordered states are AB for $0\leqslant H<H_c^1$ and A_3B for $H_c^1<H<H_c^2$, with $H_c^1=4$ and $H_c^2=12$. For $H>H_c^2$ the $T=0$ state is A with all $m_i=+1$. The phase diagram for $T=0$ confirms our expectations given in the introduction.

For $T>0$ the H-T phase diagram is more complex. The multicritical point where A, AB, and A_3B orders coexist is at $H=0$ and $T_N=3.5025$ and the transition is first order since dF/dT is discontinuous. For all $H>0$, AB order, if it occurs

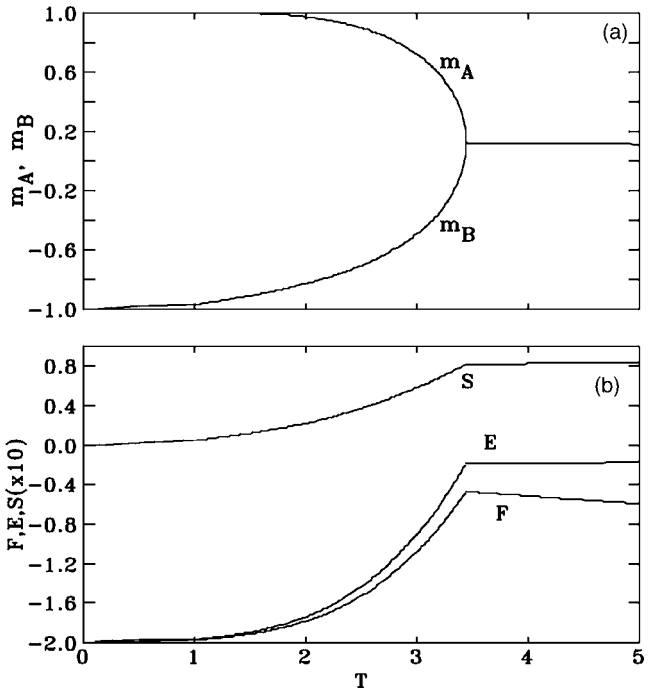

FIG. 7. Some interesting thermodynamic quantities in the ordered AB phase for $H=2$. The sublattice magnetizations m_A and m_B are shown in (a). In (b) we show, from top to bottom, the entropy/site, energy/site, and free energy/site. Note that the phase shown here becomes the solution of lowest free energy at $T_N=3.342\ldots$, below the temperature where ordered AB solutions first appear.

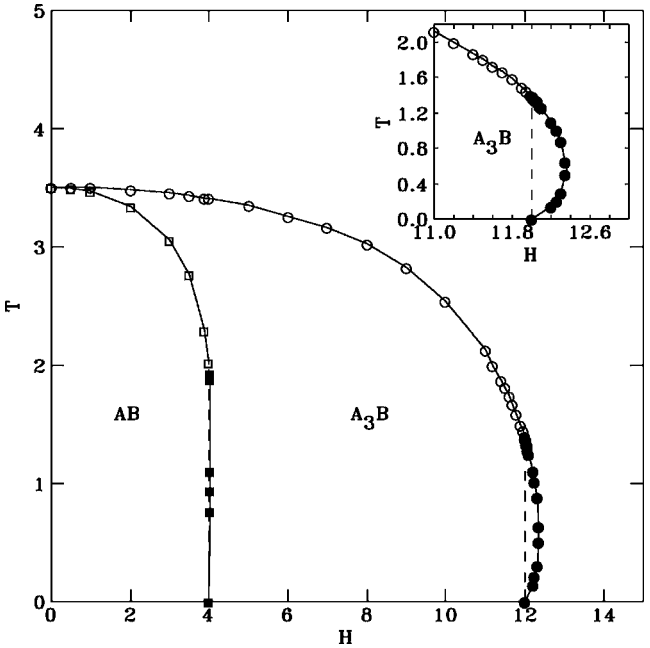

FIG. 8. Phase diagram of the fcc-IAF model studied here in the H-T plane. Closed symbols represent reentrant solutions. Inset shows detail around the reentrant phase near $H_c^2=12$, which is similar to the reentrant phase near $H_c^1=4$.

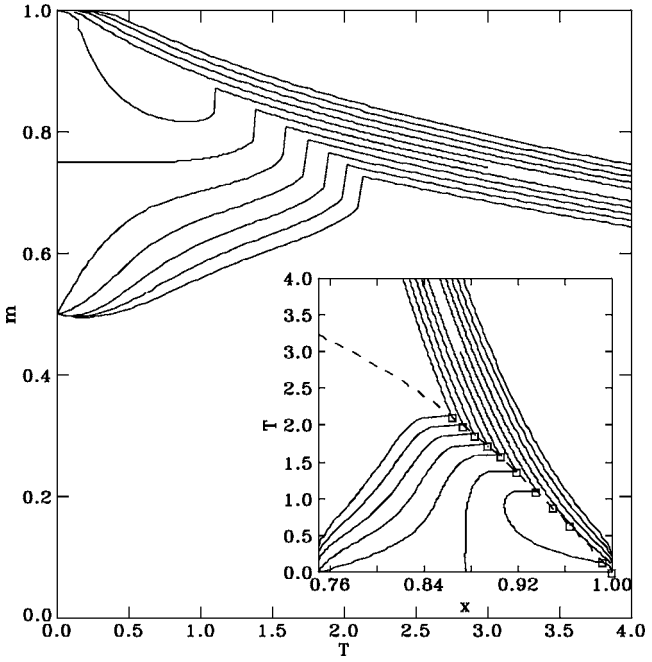

FIG. 9. Main plot shows magnetization vs temperature for fields H, in steps of $\Delta H=0.2$, from 13 to 11 from top to bottom. For $H>12$ all magnetizations approach the $T=0$ ground state A phase with $m=1$. For $4<H<12$ all magnetizations approach the A_3B ground state with $m_A=+1$ and $m_B=-1$. At $H=12$, the ordered state is A_3B with $m_A=+1$ and $m_B=0$. In the inset we show the trajectory $x(T)$ in the corresponding alloy phase diagram, and the dashed line shows the alloy phase boundary.

at all, always does so with $T_N^{AB}<T_N^{A_3B}$. The transition from the paramagnetic A state to the ordered A_3B state is first order, as there is both a jump in the sublattice magnetization at $T_N^{A_3B}$ and dF/dT is discontinuous. The ordered AB state is always entered upon decreasing temperature from an ordered A_3B state. The transition to the AB state, however, occurs at a temperature *below* that where ordered AB solutions first occur. We locate T_N^{AB} as the point where the free energy of the AB state becomes less than the free energy of the A_3B state. The transition from A_3B to AB state is also first order since there is again a jump in the sublattice magnetization and dF/dT is discontinuous.

In two rather narrow regimes, $H_c^1<H<4.05$ and $H_c^2<H<12.35$, reentrant behavior occurs. For $H_c^1<H<4.05$, upon decreasing T from the paramagnetic A state, the following sequence of transitions occurs: $A\rightarrow A_3B\rightarrow AB\rightarrow A_3B$. For $H_c^2<H<12.35$, upon decreasing T from the paramagnetic A state, the following sequence of transitions occurs: $A\rightarrow A_3B\rightarrow A$. This, perhaps surprising, occurrence of reentrant phases is actually in full agreement with the x-T phase diagram of Shockley shown in Fig. 1(a).

To understand the reentrant phases, consider the magnetization at constant H, $m_H(T)$, in the vicinity of the reentrant phase near $H_c^2=12$ as shown in Fig. 9 (a similar explanation is found for the reentrant phase near H_c^1). Upon entering the A_3B phase with decreasing T for $H<12$ the magnetization jumps downward and approaches the ordered A_3B ground state with $m=\frac{1}{2}$ ($m_A=-m_B=+1$) at $T=0$. At $H=12$ the A_3B order is different: The $T=0$ A_3B ground state with $m=\frac{3}{4}$ ($m_A=+1$ and $m_B=0$) becomes degenerate with the ordered A ($m_A=+1$) and the ordered A_3B ($m_A=+1$ and $m_B=-1$) ground states. However, the entropy of the A_3B state with $m=\frac{3}{4}$ is highest, since $\langle S_B\rangle=\langle\pm 1\rangle=0$ with equal probability, and is therefore the state selected to order. At $H=12$, cooling within the paramagnetic A state causes the magnetization to first increase and then jump downward at T_N, approaching $m=\frac{3}{4}$ at $T=0$. For $12<H<12.35$, upon cooling, the magnetization first jumps downward at T_N, looking for the intermediate $H=12$ A_3B ground state with $m=\frac{3}{4}$. However, at some lower temperature $T_{N'}$ ordered solutions no longer occur and the magnetization jumps back upward, rejoining the paramagnetic A solution which is the ground state for $H>12$. For $H>12.35$, only paramagnetic solutions occur and the magnetization smoothly approaches $m=1$ at $T=0$.

In the corresponding alloy problem the $m_H(T)$ vs T curves (Fig. 9) appear as trajectories in the x-T plane (inset to Fig. 9) with

$$x(T)=\frac{1}{2}[m(T)+1]. \tag{26}$$

The phase transitions in the x-T plane are then the loci of points $[x(T_N),T_N]$. The x-T alloy phase diagram which corresponds to the H-T magnetic phase diagram (with reentrant phases as shown in Fig. 8) is derived in the inset of Fig. 9 near $x=1$. Treating the alloy problem using a nonconserved order parameter, as we have done here, results in a x-T phase diagram which shares the same features as the Bragg-Williams phase diagram [Fig. 1(a)] with a conserved order parameter. In particular the $T=0$ critical concentrations analogous to H_c^1 and H_c^2 are found to be $x_c^1=\frac{3}{4}$ and $x_c^2=1$ as in Shockley's Bragg-Williams treatment. It would therefore appear that the LS scheme is, in some sense, equivalent to the Bragg-Williams approximation when only four spins are allowed to fluctuate. It should be noted that if one treats the alloy problem with a conserved order parameter x, and thus also m, it is not possible to know the trajectory $m_H(T)$ in the magnetic problem. Therefore, the H-T phase diagram cannot be fully reconstructed from the x-T phase diagram.

VI. DISCUSSION

The most important result of our work is the occurrence of two reentrant phases in the H-T plane. It is certainly of interest to know whether the fcc-IAF model possesses reentrance when studied without resorting to approximations. Very little analytic work has been done in the vicinity of the $T=0$ critical fields H_c^1 and H_c^2 apart from studies of the alloy problem. However, as we have shown, the absence of reentrance in the x-T phase diagram does not allow for a conclusion with regards to the absence or presence of reentrance in the H-T phase diagram. The early Monte Carlo work of Binder[5] did not find reentrance near either H_c^1 or H_c^2. On the other hand, more recent work from Binder and co-workers,[4] which focused on the multicritical point where A, AB, and A_3B phases coexist, found significant problems with the earlier work [compare Figs. 1(c) and 1(d)], and it remains a

possibility that future Monte Carlo calculations will confirm the reentrance we have found.

The possibility that reentrance may actually occur in the fcc-IAF model is supported by the observation of reentrance in simpler, but related, IAF models. The simple cubic IAF (sc-IAF) and body-centered cubic IAF (bcc-IAF) are also known to display reentrant phases near their critical fields, although the results depend on the technique used to study the models.[19] While the consensus is that the sc-IAF model does not contain a reentrant phase, a great deal of evidence exists in support of a reentrant phase for the bcc-IAF model,[19] including Monte Carlo calculations[20] and series expansions.[21] The difference in the behavior of the sc-IAF and bcc-IAF models is attributed to an increase in the lattice coordination number, with reentrance appearing in the bcc case ($z=8$) but not in the sc case ($z=6$). Since the fcc-IAF model has $z=12$, the simple trend suggests that the reentrance we have observed is not an artifact of the LS scheme we use, but a real feature of the fcc-IAF model.

The range of fields over which reentrance is observed in the bcc-IAF is reduced by about an order of magnitude in the Monte Carlo results from the mean-field predictions. If reentrance occurs in the fcc-IAF as well, then we should expect a similar reduction from our mean-field predictions, making the range of fields where reentrance occurs quite small. Reentrance in our study is limited to a $\sim 2\%$ window around H_c^1 and a $\sim 3\%$ window around H_c^2, so in a Monte Carlo calculation we expect the window to be of the order 0.2% ($4 < H < 4.008$) and 0.3% ($12 < H < 12.035$), respectively, making the reentrant phases extremely difficult to observe, especially when the behavior is unexpected. Therefore, a dedicated Monte Carlo study focused on the immediate vicinity of H_c^1 and H_c^2 would be necessary to confirm the reentrant phases we have found in our study of the fcc-IAF model.

VII. CONCLUSIONS

We have studied the fcc-IAF model using a MFT which, for the first time, shows qualitatively correct behavior, unlike two-spin MFT and the Bethe ansatz. However, our MFT disagrees with the accepted result that the multicritical point where the A, AB, and A_3B phases meet occurs at finite temperatures and field. In contrast, our method agrees with the Bragg-Williams approximation in this respect. It is important to note that our result and the Bragg-Williams result come about by completely different approximation methods: Our result is obtained by calculating the partition function and related averages in the spirit of a microscopic statistical mechanical formalism, while the Bragg-Williams result (as well as the Kikuchi result) is obtained by approximating the free-energy functional with no fluctuating degrees of freedom.

In addition, we have found that our model contains reentrance in the H-T phase diagram. However, our x-T phase diagram is equivalent to Shockley's and therefore does not contain any reentrance. This serves to highlight why the study of the magnetic problem, while often more difficult than the alloy problem, is inherently more versatile as it encompasses both the alloy and magnetic problems. Furthermore, since the method we use becomes exact as the number of fluctuating spins is increased to infinite, it will be interesting to see how the phase diagram changes when a larger cluster of fluctuating spins is included in the calculation. However, the next order of approximation consistent with the symmetry of the lattice requires 32 fluctuating spins, and would require considerably more effort than that required here. The occurrence of reentrant phases in the fcc-IAF model with magnetic field certainly deserves further attention. Given the simplicity of the model, it presents a simple place to look for the conditions necessary for reentrance to occur.

[1] G. H. Wannier, Phys. Rev. **79**, 357 (1950).
[2] L. Onsager, Phys. Rev. **65**, 117 (1944).
[3] S. Galam and P. V. Koseleff, Eur. Phys. J. B **28**, 149 (2002).
[4] S. Kämmerer, B. Dünweg, K. Binder, and M. d'Onorio de Meo, Phys. Rev. B **53**, 2345 (1996).
[5] K. Binder, Phys. Rev. Lett. **45**, 811 (1980).
[6] J. M. Luttinger, Phys. Rev. **81**, 1015 (1950).
[7] M. J. Richards and J. W. Cahn, Acta Metall. **19**, 1263 (1971).
[8] W. Shockley, J. Chem. Phys. **6**, 130 (1938).
[9] Y.-Y. Li, J. Chem. Phys. **17**, 447 (1948).
[10] R. Kikuchi and H. Sato, Acta Metall. **22**, 1099 (1974).
[11] H. A. Bethe, Proc. R. Soc. London, Ser. A **150**, 552 (1935).
[12] R. Peierls, Proc. R. Soc. London **154**, 207 (1936).
[13] C. E. Easthope, Proc. Cambridge Philos. Soc. **33**, 502 (1937).
[14] S. Galam, Phys. Rev. B **54**, 15 991 (1996).
[15] G. D. Mahan and F. H. Claro, Phys. Rev. B **16**, 1168 (1977).
[16] C. M. van Baal, Physica (Amsterdam) **64**, 571 (1973).
[17] R. Kikuchi, J. Chem. Phys. **60**, 1071 (1974).
[18] J. M. Sanchez, D. de Fontaine, and W. Teitler, Phys. Rev. B **26**, 1465 (1982).
[19] M. A. Neto and J. R. de Sousa, Phys. Rev. B **70**, 224436 (2004).
[20] D. D. Landau, Phys. Rev. B **16**, 4164 (1977).
[21] Z. Ràcz, Phys. Rev. B **21**, 4012 (1980).